Mode locking in quantum-Hall-effect point contacts

H. H. Lin
Department of Physics, University of California at Santa Barbara, Santa Barbara, California 93106

Matthew P. A. Fisher
Institute for Theoretical Physics, University of California at Santa Barbara, Santa Barbara, California 93106-4030

(Received 1 November 1995; revised manuscript received 17 July 1996)

We study the effect of an ac drive on the current-voltage (I-V) characteristics of a tunnel junction between two fractional quantum Hall fluids at filling ν^{-1} an odd integer. Within the chiral Luttinger-liquid model of edge states, the point-contact dynamics is described by a driven damped quantum mechanical pendulum. In a semiclassical limit which ignores electron tunneling, this model exhibits mode locking, which corresponds to current plateaus in the I-V curve at integer multiples of $I=e\omega/2\pi$, with ω the ac drive angular frequency. By analyzing the full quantum model at nonzero ν using perturbative and exact methods, we study the effect of quantum fluctuation on the mode-locked plateaus. For $\nu=1$, quantum fluctuations smear completely the plateaus, leaving no trace of the ac drive. For $\nu \geqslant \frac{1}{2}$ smeared plateaus remain in the I-V curve, but are not centered at the currents $I=ne\omega/2\pi$. For $\nu<\frac{1}{2}$ rounded plateaus centered around the quantized current values are found. The possibility of using mode locking in fractional quantum-Hall-effect point contacts as a current-to-frequency standard is discussed. [S0163-1829(96)06040-7]

I. INTRODUCTION

Conductance through a tunnel junction is proportional to the electron density of states in two electrodes. For metallic electrodes, which have a nonzero density of states at the Fermi energy, the tunnel junction current-voltage (I-V) characteristics are Ohmic at low bias. In marked contrast, recent theories[1,2] have predicted strongly non-Ohmic behavior for tunneling through a point contact separating two fractional quantum-Hall-effect (FQHE) fluids. Specifically, for the filling factor $\nu=1/m$, with odd integer m, the tunnel current at zero temperature is predicted to vary with voltage as $I\sim V^{2/\nu-1}$. At finite temperatures, Ohmic behavior is recovered at small voltages, with a zero-bias differential conductance varying as $dI/dV\sim T^{2/\nu-2}$. A temperature dependence consistent with this has been seen in a recent experiment by Milliken, Webb, and Umbach[3] for the tunneling conductance between two FQHE fluids at filling $\nu=\frac{1}{3}$.

The non-Ohmic tunneling conductance is due to the strange properties of the edge states in the FQHE. FQHE edge states are a beautiful realization of one-dimensional Luttinger liquids.[1] In contrast to metallic electrodes, the tunneling density of states in a Luttinger liquid *vanishes* at the Fermi energy, which leads to the vanishing tunnel conductance between two FQHE fluids. Thus, in contrast to conventional metallic tunnel junctions, a FQHE tunnel junction is an *insulator*.

An *insulating* point-contact junction is, in many respects, the dual of a superconducting point contact—namely, a Josephson junction. In a Josephson junction the I-V curve is also strongly non-Ohmic, with voltage vanishing rapidly for currents below the critical current I_J. Moreover, the zero-bias resistance is expected to vanish exponentially as $T\rightarrow$, $dV/dI\sim\exp(-E_J/k_BT)$, with energy barrier $E_J=\phi I_J$. Under exchange of current with voltage, the behavior is similar to the vanishing conductance in the FQHE point contact. In a Josephson junction, the phase difference between the superconducting electrodes is behaving classically, whereas in the FQHE junction the classical variable is the transferred electron charge.

One of the most striking manifestations of the ac Josephson effect is the presence of quantized voltage steps (Shapiro steps) in an applied microwave field[4]. The applied radiation at angular frequency ω mode locks to the discrete phase slip events leading to plateaus at voltages $V=n(\hbar/2e)\omega$, for integer n. In the plateaus, the voltage is so accurately quantized that Shapiro steps serve as a voltage-to-frequency standard.

The duality between Josephson junctions and FQHE junctions, suggests that the latter might also exhibit interesting behavior in the presence of an applied ac field. In this paper, we study in detail the effect of an ac drive on a FQHE tunnel junction, focusing on the structure induced in the I-V characteristics. One anticipates the possibility of mode locking between the ac drive and the electron-tunneling events. This could lead to steps in the junction *current*, quantized at integer multiples of $I=e\omega/2\pi$—the analog of Shapiro steps.

Quantized current plateaus for metallic tunnel junctions were proposed several years back.[5] Due to Coulomb blockade effects, it was argued that normal metal tunnel junctions with sufficiently high resistances would exhibit the phenomena of Bloch oscillations—an oscillatory voltage in the presence of a dc current—the dual of the ac Josephson effect. Moreover, it was suggested that an applied ac drive would mode lock to these oscillations, resulting in current plateaus. A more favorable geometry for current plateaus, consists of multiple-tunnel junctions in series, which can be separately tweaked by an ac drive, thereby transferring the electrons one-by-one through the circuit. Such an electron ''turnstile'' was realized experimentally, by a number of groups, both in metallic systems[6–8] and in semiconductor heterostructures.[9–11] Due to the multiple-junction geometry the tun-

stiles only work well at rather low frequencies, below tens of MHz. At higher frequencies the electrons take too long to pass across the junctions, and do not ''keep up'' with the ac drive.

In a Josephson junction, Shapiro steps are very robust, and do not need complicated multiple-junction geometries. Moreover, Shapiro steps are observed up to frequencies comparable to the superconducting gap. The reason for this is that the junction phase difference is a classical field, so that phase-slip processes are classical events which readily lock to an ac drive. In ''insulating'' FQHE point contacts the electron charge is a good quantum number, which suggests that mode locking might also be possible in a single-junction configuration. However, quantum fluctuations in the electron charge transfer are expected to be more important than quantum phase-slip processes in the Josephson junction, as reflected in the power-law voltage and temperature dependences in the *I-V* curves of the FQHE junction. (Because the phase of the superconducting wave function exhibits true long-ranged order, low-frequency quantum phase slips are expected to be completely absent.) This paper is devoted to studying the effect of such quantum fluctuations in washing out mode-locked steps.

The organization and central results of the paper are as follows. In Sec. II we introduce the edge-state model for a FQHE tunnel junction at filling $\nu=1/m$, in the presence of both a dc source-to-drain voltage $V_{\rm sd}$ and an ac drive voltage, $V_{\rm ac}\sin\omega t$. While the model is only appropriate for FQHE edges when ν^{-1} is an odd integer, it is well defined for general ν.

In Sec. III we consider a semiclassical limit, which ignores quantum tunneling of the electron. In this limit, the model reduces to the classical dynamics of a periodically driven overdamped pendulum, with the phase of the pendulum representing the charge transferred across the junction. This classical model is equivalent to the resistively-shunted junction (RSJ) model of Josephson-junction dynamics.[12–14] Not surprisingly, robust mode-locked current plateaus are found in this semiclassical limit.

In Sec. IV we study the full quantum model, and derive exact solutions for the *I-V* curves at two special values $\nu=1$ and $\frac{1}{2}$. At $\nu=1$, appropriate for the integer quantum Hall effect, quantum fluctuations are so strong that *all* of the mode-locked structure in the *I-V* curves is completely wiped out. For $\nu=\frac{1}{2}$, the solution reveals the remaining structure, but the smeared current plateaus are *not* centered at integer multiples of $I=e\omega/2\pi$.

In Sec. V we compute the *I-V* curves in a perturbative approach, which leads us to conjecture the following general form for the *I-V* curves at arbitrary ν:

$$I(V_{\rm sd},V_{\rm ac})=\sum_n |c_n|^2 \; I^{\rm dc}(\nu V_{\rm sd}+n\omega). \tag{1.1}$$

Here $I^{\rm dc}(V)\equiv I(V,0)$ is the tunnel current in the absence of the ac drive, and $|c_n|^2=|J_n(\nu V_{\rm ac}/\omega)|^2$, with $J_n(X)$ nth-order Bessel functions. These coefficients satisfy the sum rule $\Sigma_n|c_n|^2=1$. This form has a simple physical interpretation: Charge ν quasiparticles absorb n quanta from the ac field with probability $|c_n|^2$, and are transmitted through the point contact with total energy $\nu V_{\rm sd}+n\omega$.

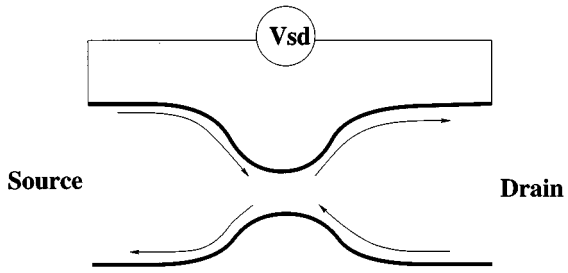

FIG. 1. Schematic representation of a point contact in a FQHE fluid. The lines with arrows represent edge states which can scatter at the point contact. The voltage drop between source and drain is denoted $V_{\rm sd}$.

Equation (1.1), which is also consistent with our exact solutions, gives a simple explanation as to why all plateaus are wiped out at $\nu=1$. For $\nu=1$ the edge states are describable in terms of noninteracting electrons (Fermi liquid). Under the assumption of an energy independent transmission probability through the junction, the dc *I-V* curves are linear (Ohmic). Since the transmission is independent of energy, the ac drive has *no* effect on the *I-V* curves, which remain completely linear.

For $\nu<1$ the dc *I-V* curves are non-linear, and plateau-like features show up with an ac drive. Recently, Fendley, Ludwig, and Saleur[15] obtained exact solutions for the dc *I-V* curve at arbitrary integer ν^{-1}. These curves, together with conjecture (1.1), enable us to construct *I-V* curves with ac drive present for the experimentally relevant cases of $\nu=\frac{1}{3}$ and $\frac{1}{5}$. For these cases, in the limit of weak pinchoff at the point contact, the *I-V* curves exhibit smeared current plateaus centered at integer multiples of $I=e\omega/2\pi$. Section VI is devoted to a discussion of the experimental consequences.

II. MODEL FOR POINT CONTACT WITH ac DRIVE

Consider a FQHE state at filling ν^{-1} an odd integer. For this class of Hall fluids only a single-edge mode is expected.[1] For the IQHE at $\nu=1$, a free-fermion description of the edge mode is possible,[16] but more generally the edge mode is expected to be a (chiral) Luttinger liquid, describable in terms of a bosonic field.

Let ρ_R and ρ_L denote the electron densities in the right- and left-moving edge modes, on the top and bottom of the sample, as shown schematically in Fig. 1. These densities are written as gradients of bosonic fields,

$$\rho_{R/L}=\pm\frac{1}{2\pi}\partial_x\phi_{R/L}, \tag{2.1}$$

which satisfy the Kac-Moody commutation relations[1]

$$[\phi_{R/L}(x),\partial_x\phi_{R/L}(x')]=\mp i2\pi\nu\delta(x-x'). \tag{2.2}$$

Here x is a one-dimensional position coordinate, running along the edge. The appropriate Hamiltonian density describing the propagation of edge modes is[16,2]

$$\mathcal{H}_0=\frac{v_F}{4\pi\nu}[(\partial_x\phi_R)^2+(\partial_x\phi_L)^2]. \tag{2.3}$$

Here v_F is the velocity of edge propagation.

At the point contact, the right- and left-moving edge modes are brought into close proximity, and tunneling between them becomes possible. In the limit of weak tunneling, the dominant backscattering process at low temperatures is of fractionally charged ($Q=e\nu$) Laughlin quasiparticles.[17] The appropriate tunneling term is

$$\mathcal{H}_1 = v\,\delta(x)[e^{i(\phi_R-\phi_L)}+\text{H.c.}], \tag{2.4}$$

where v is the local tunneling amplitude, at the point contact, $x=0$.

In the presence of an applied source-to-drain voltage, the incoming edge modes will be at different chemical potentials. Interedge tunneling processes will thus change the energy. Denoting the applied voltage as $V(t)$, the energy change can be written

$$\mathcal{H}_V = (\rho_R-\rho_L)\tfrac{1}{2}V(t). \tag{2.5}$$

In addition to a dc source-to-drain voltage $V_{\rm sd}$, we will consider an applied ac field, arising from electromagnetic radiation illuminating the point contact. The total voltage drop between edges is written

$$V(t) = V_{\rm sd}+V_{\rm ac}\sin\omega t. \tag{2.6}$$

For later convenience it will be useful to introduce a gauge field $A(t)$, defined via $V(t)=\partial_t A(t)$. A useful identity is

$$e^{i\nu A(t)} = e^{i\nu V_{\rm sd}t}\sum_{n=-\infty}^{\infty} c_n e^{-in\omega t}, \tag{2.7}$$

where $c_n=(-i)^n J_n(\nu V_{\rm ac}/\omega)$, with $J_n(X)$ Bessel functions. The full Hamiltonian density is $\mathcal{H}=\mathcal{H}_0+\mathcal{H}_1+\mathcal{H}_V$.

In the absence of backscattering at the point contact, the total source-to-drain current $I=v_F(\rho_R-\rho_L)$, upon averaging over time, is appropriately quantized $\langle I\rangle=\nu V_{\rm sd}/2\pi$. Backscattering will reduce this current to

$$\langle I\rangle = \frac{1}{2\pi}\nu V_{\rm sd}-\langle I_B\rangle, \tag{2.8}$$

where I_B is the backscattering current operator. An expression for I_B follows upon functional differentiation,

$$I_B \equiv -\frac{\delta H}{\delta A} = \partial_t \frac{1}{2}\int dx(\rho_R-\rho_L). \tag{2.9}$$

For later convenience it will be useful to define additional boson fields which propagate in the same direction,

$$\phi_1(x)\equiv\phi_R(x), \quad \phi_2(x)\equiv\phi_L(-x). \tag{2.10}$$

The commutators become

$$[\phi_i(x),\partial_x\phi_j(x')] = -i\delta_{ij}2\pi\nu\delta(x-x'). \tag{2.11}$$

The Hamiltonian density has the same form as before,

$$\mathcal{H} = \frac{v_F}{4\pi\nu}(\partial_x\phi_i)^2 + v\,\delta(x)[e^{i(\phi_1-\phi_2)}+\text{H.c.}] + (\rho_1-\rho_2)\tfrac{1}{2}V(t), \tag{2.12}$$

provided the densities are defined as, $\rho_i=\partial_x\phi_i/2\pi$. Upon using the continuity equations $\partial_t\rho_i+v_F\partial_x\rho_i=0$, valid away from the point contact at $x=0$, the backscattering current operator can be reexpressed as

$$I_B = -(v_F/2)\int dx\,\partial_x(\rho_1-\rho_2) = (v_F/2)(\rho_1-\rho_2)\big|_{x=0^-}^{x=0^+}. \tag{2.13}$$

Here we have used the fact that the only backscattering is at the origin $x=0$.

It is worth emphasizing that the above model is only appropriate for a FQHE point contact at filling factor ν^{-1} an odd integer. For FQHE states at other filling factors, multiple edge modes are expected. Nevertheless, it will prove useful below to study the above model for arbitrary ν.

The current voltage characteristics of the point contact follow upon computing the backscattering current (2.13). Before attempting this, we consider briefly a semiclassical limit of the model which describes an overdamped driven classical pendulum. Under exchange of current with voltage, this is identical to the standard RSJ model of Josephson-junction dynamics.[12–14] This classical model has been studied intensively, both because of its relevance to Josephson junctions and as a simple example of a classical dynamical system which exhibits mode locking and a devil's staircase.[19]

III. SEMICLASSICAL LIMIT

To take the semiclassical limit we first review the equivalence between the quantum Hall point contact and the Caldeira-Leggett model[20] for the quantum mechanics of a damped pendulum. To this end, it is first useful to perform a gauge transformation to eliminate $\mathcal{H}_V$ in Eq. (2.5). Since the equations of motion for $x\neq 0$ take the form

$$(\partial_t \pm v_F\partial_x)\phi_{R/L} = \pm\frac{\nu}{2}V(t), \tag{3.1}$$

this can be achieved via the transformation

$$\phi_{R/L}\rightarrow\phi_{R/L}\pm\frac{\nu}{2}A(t). \tag{3.2}$$

After the gauge transformation, the full Hamiltonian reads

$$\mathcal{H} = \frac{v_F}{4\pi\nu}[(\partial_x\phi_R)^2+(\partial_x\phi_L)^2]+v\,\delta(x)\cos(\phi_R-\phi_L+\nu A). \tag{3.3}$$

Since the interaction term only depends on the difference, $\phi_R-\phi_L$, it is useful to define additional fields

$$\varphi=\phi_R+\phi_L, \quad \theta=\phi_R-\phi_L. \tag{3.4}$$

Since the transformed Hamiltonian is quadratic in φ, it can be integrated out, giving, for the Euclidean Lagrangian,

$$\mathcal{L}_E = \frac{1}{8\pi\nu}(\partial_\mu\theta)^2+v\,\delta(x)\cos(\theta+\nu A). \tag{3.5}$$

Here we have set $v_F=1$ in the first term. Finally, upon integrating out $\theta(x)$ for $x\neq 0$, we arrive at an effective Euclidean action in terms of $\theta(x=0,\tau)$:

$$S_E=\frac{1}{4\pi\nu}\int\frac{d\omega}{2\pi}\ |\omega||\theta(\omega)|^2+\int d\tau\ v\ \cos(\theta+\nu A). \tag{3.6}$$

This action can be recognized as a Caldeira-Leggett model of a damped driven quantum pendulum.[20] It should be emphasized that the Ohmic damping that characterizes the Caldeira-Leggett model can be traced to the one-dimensional (1D) Luttinger-liquid behavior of the edge modes. Although this model has been used to describe quantum dynamics in Josephson junctions, it is unclear that it describes the appropriate low-frequency dynamics. In particular, the phase of the Cooper pair field has long-ranged order in the bulk superconducting electrodes, in contrast to the power-law correlations described by the 1D edge modes in Eqs. (2.3).

Since we are interested in the nonequilibrium current-voltage characteristics, we need a real-time formulation, such as Keldysh.[21] In the Keldysh approach a generating functional is introduced as a path-integral sum over two paths propagating forward and backward in time, $\theta_\pm(t)$:

$$Z=\int D[\theta_+]D[\theta_-]\ \ e^{-S(\theta_\pm)}. \tag{3.7}$$

In terms of additional fields,

$$\theta(t)=\tfrac{1}{2}[\theta_+(t)+\theta_-(t)],\quad \widetilde{\theta}(t)=\theta_+(t)-\theta_-(t) \tag{3.8}$$

the appropriate real-time action is $S=S_0+S_1$, with

$$S_0=\frac{1}{2}\int d\omega\alpha_R(\omega)|\widetilde{\theta}(\omega)|^2-\frac{i}{2\pi\nu}\int dt\ \dot{\theta}\widetilde{\theta}, \tag{3.9}$$

$$S_1=\sum_{\pm}\int dt(\pm iv)\cos(\theta\mp\tfrac{1}{2}\widetilde{\theta}+\nu A). \tag{3.10}$$

Here we have defined $\alpha_R(\omega)=(\omega/2\pi\nu)\coth(\frac{1}{2}\beta\omega)$. The above gives a general quantum-mechanical formulation of the model. To complete the description we must identify the source-to-drain current operator. From Eq. (3.4) we see that $\theta(x=0)=2\pi\int_{-\infty}^{0}\rho_{\rm tot}dx$, where $\rho_{\rm tot}=\rho_R+\rho_L$. Thus $\theta(x=0)/2\pi$ can be identified as the total charge to the left of the point contact. The source-to-drain current through the point contact is thus simply

$$I=\partial_t\theta(x=0,t)/2\pi. \tag{3.11}$$

An instanton in $\theta(t)$ of magnitude 2π corresponds to the transfer of one electron through the point contact. In the classical limit these charge-transfer processes occur over the barrier, rather than by quantum-mechanical tunneling. In the Keldysh formulation, quantum tunneling processes correspond to instantons in $\widetilde{\theta}(t)$—in which only the forward path tunnels, say. Thus the semiclassical limit can be obtained by forbidding such processes. This can be implemented by expanding the cosines in Eq. (3.10) for small $\widetilde{\theta}$, and retaining only the leading term

$$S_1=iv\int dt\ \widetilde{\theta}\ \sin(\theta+\nu A)+O(\widetilde{\theta}^3). \tag{3.12}$$

This expansion destroys the periodicity in $\widetilde{\theta}$. The full action can now be written

$$S=\tfrac{1}{2}\int d\omega\ \alpha_R(\omega)|\widetilde{\theta}(\omega)|^2-i\int dt\times\widetilde{\theta}\left[\frac{1}{2\pi\nu}\dot{\theta}-v\ \sin(\theta+\nu A)\right], \tag{3.13}$$

which can be recognized as the Martin-Siggia-Rose action for a classical stochastic differential equation.[22] Upon introducing a stochastic noise term $\xi(t)$, the action can be reexpressed as

$$S=\tfrac{1}{2}\int d\omega\ \frac{1}{\alpha_R(\omega)}|\xi(\omega)|^2-i\int dt\ \widetilde{\theta}\left[\frac{1}{2\pi\nu}\dot{\theta}-v\ \sin(\theta+\nu A)-\xi(t)\right]. \tag{3.14}$$

The integration over $\widetilde{\theta}$ then gives a δ function, enforcing the classical equation of motion

$$\frac{1}{2\pi\nu}\dot{\theta}=v\ \sin(\theta+\nu A)+\xi(t) \tag{3.15}$$

with stochastic noise

$$\langle|\xi(\omega)|^2\rangle=\frac{\omega}{2\pi\nu}\coth(\tfrac{1}{2}\beta\omega). \tag{3.16}$$

A final gauge transformation $\theta\to\theta-\nu A$ brings the equation into the familiar form,

$$\frac{1}{2\pi}\dot{\theta}=\nu v\ \sin(\theta)+\frac{\nu}{2\pi}V(t)+\nu\xi(t). \tag{3.17}$$

Under exchange of current and voltage, Eq. (3.17) becomes equivalent to the equation which describes Josephson junctions,[12–14] except for the colored stochastic noise term which is non-vanishing even at zero temperature. However, if we take the semiclassical limit $\nu\to0$, with νv and $\nu V(t)$ held fixed, the noise term drops out. In this classical limit, the FQHE point contact is exactly dual to a Josephson junction, and should exhibit similar mode locking under exchange of current and voltage. Solutions of Eq. (3.17) in the noiseless limit are well known.[23–25] For a Josephson junction they give mode-locked voltage plateaus at integer multiples of $V=(\hbar/2e)\omega$. Physically, there is a mode locking between the discrete phase slip events and the ac drive. For the FQHE point contact, the mode-locked plateaus are in the current, at integer multiples of $I=e2\pi\omega$. The discrete process is an electron tunneling through the point contact.

After rescaling the time in Eq. (3.17) via $t\to\omega t$, it is clear that the I-V curves are characterized by two independent dimensionless parameter $2\pi\nu v/\omega$ and $\nu V_{\rm ac}/\omega$. Representative current-voltage characteristics computed numerically from (3.17) in the noiseless limit are shown in Fig. 2. As expected, the I-V curves exhibit plateaus in the current which are ''flat'' and quantized at integer multiples of $I=e\omega/2\pi$. Subharmonic plateaus are absent for model (3.17), but would be present if the periodic function $\sin(\theta)$ included higher harmonic content.[26]

With inclusion of stochastic noise, one anticipates that these plateaus will be rounded slightly, as shown in the I-V

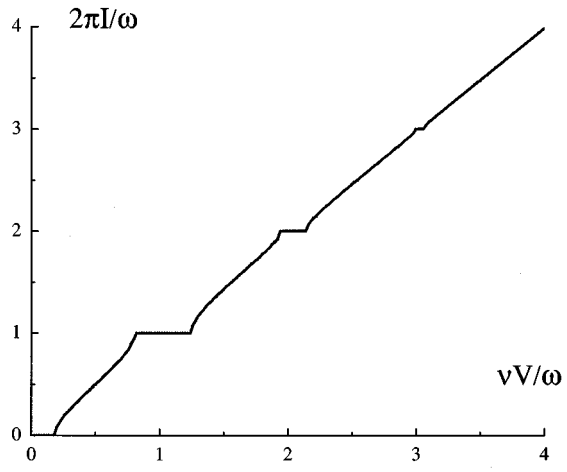

FIG. 2. Current voltage characteristic within the semiclassical approximation, obtained from Eq. (3.17) with no stochastic noise. Both the current and voltage are plotted in units of the ac drive frequency. The backscattering amplitude has been chosen to be $2\pi\nu v=\omega/4$ and the ac drive amplitude is $\nu V_{\rm ac}=1.6\omega$. Notice the current plateaus at integer multiples of $I=e\omega/2\pi$, indicating a mode locking to the ac drive.

curves in Fig. 3, obtained by numerically integrating Eq. (3.17) with colored noise. When the noise is weak, the rounding is most visible at the edges of the plateaus. For large enough noise the plateaus become completely smeared out. The effects of colored noise are qualitatively similar to stochastic white noise, which has been studied extensively in the past.

It is worth commenting here on the validity of the semiclassical approximation to the full quantum dynamics. As evident from Eq. (3.12), the semiclassical approximation involves discarding all electron-tunneling events, in which $\tilde{\theta}$ changes by 2π. One can argue from the quadratic action (3.9) that the typical variance of $\tilde{\theta}$ is proportional to ν, even

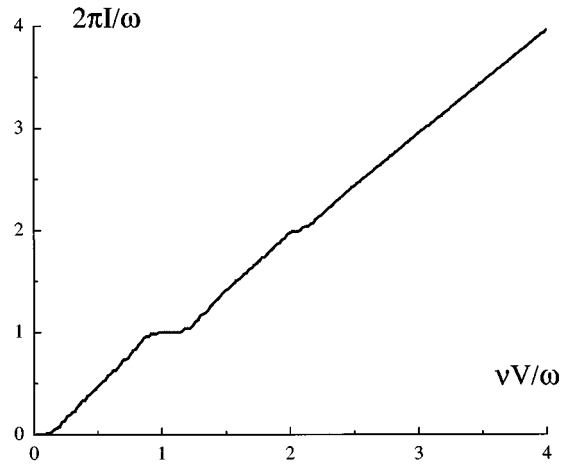

FIG. 3. An I-V curve in the semiclassical approximation, obtained from Eq. (3.17) with stochastic colored noise. As in Fig. 2, we choose $2\pi\nu v=\omega/4$ and $\nu V_{\rm mac}=1.6\omega$. The colored noise has strength $\nu=0.1$ and the cutoff frequency for generating the noise is $\omega_c=60\omega$. Notice that the current plateaus are rounded, due to the presence of the stochastic noise.

when $v=0$: $\tilde{\theta}^2\sim\nu\ \ln(\omega_c/T)$, with cutoff frequency ω_c. This suggests that the semiclassical expansion in Eq. (3.12) might become exact in the $\nu\to 0$ limit. In the absence of an ac drive this is in fact the case. Recently, Fendley, Ludwig, and Saleur obtained exact I-V curves, with no ac drive, for arbitrary odd integer ν^{-1}. One can analyze these I-V curves in the limit $\nu\to 0$, with νv and νV held fixed. In this limit, the I-V curves become equivalent to those which follow from the classical equation of motion (3.17), with white noise replacing the stochastic colored noise.

However, with an ac drive present, it is unlikely that the $\nu\to 0$ limit is equivalent to the semiclassical limit (3.17). With ac drive present there are two parallel processes which allow charge to be transported across the junction. In addition to electron tunneling ''under the barrier,'' the electron can absorb quanta of energy from the ac drive field. Once the electron energy is high enough, it can pass over the washboard barrier. In the classical limit, both of these processes are modified: Electron tunneling is suppressed completely, and energy is not absorbed from the ac drive in discrete quanta. However, in the $\nu\to 0$ limit, while the electron tunneling is also completely suppressed (since $I\sim V^{2/\nu-1}\to 0$ as $\nu\to 0$), energy is still absorbed in discrete quanta from the ac drive. Thus, once the ac drive is present, one anticipates that mode-locking features obtained from the semiclassical limit (3.17) will *not* serve as a good guide for the full quantum model, even for very small ν. This will be confirmed by more detailed analysis in Sec. V below.

IV. EXACT SOLUTIONS FOR $\nu=1, \frac{1}{2}$

In this section we study the full quantum dynamics for two special values of ν, for which simple exact solutions are possible. For $\nu=1$ the edge mode is equivalent to a free fermion.[16] When the ac drive is present, an exact solution for the I-V curve is possible. When $\nu=\frac{1}{2}$ a free-fermion representation is also possible.[18] Although the theory is not directly applicable to the FQHE edge states for $\nu=\frac{1}{2}$, the exact solution is nevertheless illuminating, revealing plateaulike structure in the I-V curve, in contrast to $\nu=1$ (see below). Moreover, the general structure of the solutions in these two soluble cases, leads to a natural conjecture for more general ν, discussed in Sec. VI.

A. $\nu=1$ solution

For $\nu=1$ the edge modes have a free-fermion description, simpler than the general bosonized representation of Sec. II. Upon defining fermion fields for the two modes,

$$\Psi=\begin{pmatrix}\psi_1\\ \psi_2\end{pmatrix}=\frac{1}{\sqrt{a_0}}\begin{pmatrix}e^{i\phi_1}\\ e^{i\phi_2}\end{pmatrix}, \tag{4.1}$$

with a_0 a short-length-scale cutoff, the full bosonized Hamiltonian can be expressed as a quadratic fermion theory

$$\mathcal{H}=-\Psi^\dagger[i\partial_x+\tfrac{1}{2}V(t)\boldsymbol{\sigma}_z]\Psi+\frac{v}{\omega_c}\delta(x)\Psi^\dagger\boldsymbol{\sigma}_x\Psi. \tag{4.2}$$

Here, we have put the Fermi velocity $v_F=1$, and the cutoff frequency $\omega_c\sim 1/a_0$. The backscattered current (2.13) takes the simple form

$$I_B = \tfrac{1}{2}\Psi^\dagger \boldsymbol{\sigma}_z \Psi|_{x=0^-}^{x=0^+}. \tag{4.3}$$

The equation of motion which follows from the fermion Hamiltonian is

$$\left[\partial_t + \partial_x - \frac{i}{2}V(t)\boldsymbol{\sigma}_z\right]\Psi = -i\frac{v}{\omega_c}\delta(x)\boldsymbol{\sigma}_x\Psi. \tag{4.4}$$

The I-V curve can be obtained by solving this equation, with appropriate boundary conditions, and extracting the backscattered current I_B.

Our solution proceeds in two steps. Away from the point contact at $x=0$, the equation describes free propagation with a uniform time-dependent potential $V(t)$. This can be eliminated by defining a gauge-transformed fermion field, which is assumed to be incident upon the point contact with a Fermi-Dirac distribution. Upon transforming back to the original Fermion field, the Fermi distribution function is modified, involving a sum over processes involving absorption and emission of the ac field. We refer to this distribution as an ''excited Fermi function.'' At the point contact ($x=0$), backscattering takes place, which is characterized by reflection and transmission coefficients (an S matrix) which are independent of the incident distribution function. The total backscattered current I_B is an appropriate convolution of the S *matrix* with the ''excited Fermi'' distribution function.

Consider first scattering at the point contact. The **S** matrix relates the incoming field Ψ_- to the outgoing field Ψ_+ via

$$\Psi_+ = \mathbf{S}\Psi_-, \tag{4.5}$$

where $\Psi_\pm(t) = \Psi(x=0^\pm, t)$. Integrating the equation of motion (4.4) through the origin, $x=0$, gives

$$\Psi_+(t) - \Psi_-(t) = -i\frac{v}{\omega_c}\boldsymbol{\sigma}_x\Psi(0,t), \tag{4.6}$$

where $\Psi(0,t) = \frac{1}{2}[\Psi_+(t) + \Psi_-(t)]$.

From this one readily obtains the **S** matrix

$$S_{11} = S_{22} = \frac{1-(v/2\omega_c)^2}{1+(v/2\omega_c)^2}, \tag{4.7}$$

$$S_{12} = S_{21} = \frac{-iv/\omega_c}{1+(v/2\omega_c)^2}. \tag{4.8}$$

The probability for the incoming field to be scattered from one edge to the other is $|S_{12}|^2$, whereas $|S_{11}|^2$ is the probability to be transmitted without scattering. Probability conservation dictates a unitary S matrix, $\mathbf{S}^\dagger\mathbf{S} = \mathbf{1}$, which is satisfied here. Notice that the S matrix is independent of the energy of the incident carriers, a consequence of the assumed δ-function point scatterer.

Outside the scattering region, the right side of Eq. (4.4) vanishes. Transforming to another fermion field

$$\Psi(x,t) = e^{(i/2)A(t)\boldsymbol{\sigma}_z}\widetilde{\Psi}(x,t), \tag{4.9}$$

with $V(t) = \partial_t A(t)$ as before, then eliminates the time dependence. This field satisfies the simple wave equation $(\partial_t + \partial_x)\widetilde{\Psi} = 0$, which describes free fermions at zero chemical potential. This field is assumed to be incident with an ordinary Fermi distribution function,

$$\langle \widetilde{\psi}_i(E)^\dagger \widetilde{\psi}_i(E')\rangle = 2\pi\delta(E-E')f(E), \tag{4.10}$$

where $f(E) = (\exp(\beta E)+1)^{-1}$ and $\widetilde{\Psi}(E)$ denotes the Fourier transform of $\widetilde{\Psi}(x=0^-, t)$.

The distribution function for the original incident Fermion $\Psi_-(t)$ can now be obtained by relating the transform $\Psi_-(E)$ to $\widetilde{\Psi}(E)$ using Eq. (4.9) and the expansion (2.7). This gives

$$\psi_{1,2}^-(E) = \sum_n c_n \widetilde{\psi}_{1,2}(E - n\omega \pm \tfrac{1}{2}V_{\rm sd}), \tag{4.11}$$

where c_n is defined in Eq. (2.7). The distribution function for the original Fermion, $\langle \psi_j^{-\dagger}(E)\psi_j^-(E')\rangle = 2\pi\delta(E-E')f_j^{\rm ex}(E)$, then takes the simple form

$$f_{1,2}^{\rm ex} = \sum_n |c_n|^2 f(E - n\omega \pm \tfrac{1}{2}V_{\rm sd}), \tag{4.12}$$

an ''excited Fermi function.'' Notice that the dc voltage $V_{\rm sd}$ simply causes a shift in the energy of the incident electron. The ac drive shifts the energy by $n\omega$, corresponding to absorption or emission of n quanta, with probability $|c_n|^2$.

Finally we can obtain the backscattered current from Eq. (4.3), which can be reexpressed using Eq. (4.5) solely in terms of the incident fields as $I_B = -|S_{12}|^2\Psi_-^\dagger\boldsymbol{\sigma}_z\Psi_-$. After Fourier transforming to energy, this becomes

$$\langle I_B\rangle = -\int_{E,E'} e^{-i(E-E')t}|S_{12}|^2\langle\Psi_-^\dagger(E')\boldsymbol{\sigma}_z\Psi_-(E)\rangle. \tag{4.13}$$

In addition to a time-independent piece, the backscattered current will have oscillatory contributions at multiple frequencies of ω, as is apparent from Eq. (4.13). We focus only on the time-independent piece, which is finally given by

$$\langle I_B\rangle_{\rm time} = \frac{1}{2\pi}\int dE\ |S_{12}|^2[f_2^{\rm ex}(E) - f_1^{\rm ex}(E)]. \tag{4.14}$$

This result takes a familiar form, involving an energy integral of the reflection probability, weighted by energy distribution functions. Due to the ac drive, however, these are not simply Fermi functions, but rather the ''excited Fermi functions'' given in Eq. (4.12).

Since the reflection probability is energy independent, the backscattered current can be seen to be completely independent of the ac drive. This follows by inserting the distribution function (4.12), and shifting the energy of integration to eliminate the drive frequency ω. Since $\Sigma_n|c_n|^2 = 1$, the backscattered current is then exactly equal to the result without any ac drive present. At zero temperature this gives $\langle I_B\rangle_{\rm time} = (1/2\pi)|S_{12}|^2 V_{\rm sd}$, or for the total transmitted current [using Eq. (2.8)] upon restoring units

$$I = \frac{e^2}{h}|S_{11}|^2 V_{\rm sd}. \tag{4.15}$$

The I-V curve is linear, with conductance given by the transmission probability, just as without any ac drive. The quan-

tum fluctuations have completely washed out the current plateaus seen in the semiclassical limit of Sec. III. The absence of structure in the I-V curve can be traced to the energy-independent transmission probability. The ac drive changes the energy of the incident electron, via absorption or emission of quanta, but since the transmission probability is energy independent, this has no effect on the net transmitted current.

It is worth mentioning that the total transmitted current can be cast into the suggestive form

$$I(V_{\rm sd},V_{\rm ac})=\sum_n |c_n|^2 I^{\rm dc}(\nu V_{\rm sd}-n\omega), \tag{4.16}$$

where $I^{\rm dc}(V)\equiv I(V,0)$ is the current in the absence of an ac drive. As we shall now show, this form also holds when $\nu=1/2$, even though in that case $I^{\rm dc}(V)$ shows non-Ohmic structure. Moreover, as discussed in Sec. V, this form is also valid perturbatively in the weak backscattering limit, for general ν.

B. $\nu=\frac{1}{2}$ solution

Now consider model (2.12) with $\nu=\frac{1}{2}$. In this case one can show using the commutation relations (2.11), that the operator $\exp(\phi_1-\phi_2)$, which enters into the Hamiltonian, satisfies Fermi statistics. In order to fermionize this operator, it is convenient to define additional boson fields[15,18]

$$\phi(x,t)=[\phi_1(x,t)-\phi_2(x,t)], \tag{4.17}$$

$$\Phi(x,t)=[\phi_1(x,t)+\phi_2(x,t)]. \tag{4.18}$$

When the Hamiltonian (2.12) is reexpressed in terms of these fields, the field Φ decouples and can be ignored. The remaining Hamiltonian becomes

$$\mathcal{H}=\frac{v_F}{4\pi}(\partial_x\phi)^2+v\,\delta(x)[e^{i\phi}+\text{H.c.}]+\tfrac{1}{2}V(t)(\partial_x\phi), \tag{4.19}$$

where we have set $\nu=\frac{1}{2}$.

Since $e^{i\phi}$ has Fermi statistics, we can fermionize the remaining boson field, via $\Psi=(1/\sqrt{a_0})e^{i\phi}$, with lattice cutoff a_0. The first term describes a free chiral fermion, and the third term is also quadratic in Ψ; however, the tunneling term is *linear* in Ψ. To convert this term into a quadratic form, we introduce a local fermion field a as

$$\Psi(x)=(a+a^\dagger)\psi(x), \tag{4.20}$$

where both a and $\psi(x)$ satisfy fermion anticommutation relations. The full Hamiltonian then becomes

$$\mathcal{H}=\psi^\dagger(i\partial_x+\tfrac{1}{2}V(t))\psi+\frac{v}{\sqrt{\omega_c}}\delta(x)[\psi^\dagger(a+a^\dagger)+\text{H.c.}]. \tag{4.21}$$

Here we have set $v_F=1$, and the cutoff frequency $\omega_c\sim 1/a_0$. To complete the fermionization, we reexpress the backscattering current from Eq. (2.13) in terms of the fermion fields

$$I_B=\tfrac{1}{2}\psi^\dagger\psi|_{x=0-}^{x=0+}. \tag{4.22}$$

Since the Hamiltonian (4.21) is quadratic, it can be readily solved, and the current computed, as we now show.

To this end, consider first the equations of motion for the fermion fields which follow from the Hamiltonian. The local fermion satisfies

$$\partial_t(a+a^\dagger)=2i\frac{v}{\sqrt{\omega_c}}[\psi(0)-\psi^\dagger(0)], \tag{4.23}$$

with $\psi(0)=(\psi(x=0^+)+\psi(x=0^-))/2$, whereas $\psi(x,t)$ satisfies

$$\left[\partial_t+\partial_x-\frac{i}{2}V(t)\right]\psi=i\frac{v}{\sqrt{\omega_c}}\delta(x)(a+a^\dagger). \tag{4.24}$$

We now proceed by direct analogy with the $\nu=1$ case. Away from the point contact, the right side of Eq. (4.24) vanishes, and the time-dependent potential $V(t)$ can be eliminated by gauge transforming to another field. At the point contact, we compute the S matrix, which relates the amplitude of the incoming fermion ($x=0^-$) to the outgoing fermion ($x=0^+$).

To compute the S matrix, first integrate Eq. (4.24) through the origin ($x=0$), and then eliminate the local fermion term $a+a^\dagger$ using Eq. (4.23). This gives the local equation

$$\partial_t(\psi_+-\psi_-)=\frac{v^2}{\omega_c}\,[\psi_+^\dagger+\psi_-^\dagger-\psi_+-\psi_-], \tag{4.25}$$

where we have defined incoming and outgoing fields $\psi_\pm(t)=\psi(x=0^\pm,t)$. This can be converted to an algebraic equation by Fourier transformation

$$\psi_+(E)-\psi_-(E)=\frac{v^2}{iE\omega_c}[\psi_+(E)+\psi_-(E)-\psi_+^\dagger(-E)-\psi_-^\dagger(-E)]. \tag{4.26}$$

Upon combining this equation with its Hermitian conjugate, we can eliminate $\psi_+^\dagger(-E)$, and express the outgoing field $\psi_+(E)$ in terms of the incoming fields $\psi_-(E)$ and $\psi_-^\dagger(-E)$,

$$\psi_+(E)=S_{++}(E)\psi_-(E)+S_{+-}(E)\psi_-^\dagger(-E). \tag{4.27}$$

Here the energy-dependent S-matrix elements are given by

$$S_{++}(E)=\frac{\alpha_E}{\alpha_E+i},\quad S_{+-}(E)=\frac{i}{\alpha_E+i}, \tag{4.28}$$

with $\alpha_E\equiv E\omega_c/2v^2$. As required by current conservation, the S matrix satisfies $|S_{++}(k)|^2+|S_{+-}(k)|^2=1$.

To obtain the distribution function for the incident fermion, we follow the procedure used for $\nu=1$, and define a fermion field which eliminates the time-dependent potential in Eq. (4.24):

$$\psi(x,t)=e^{(i/2)A(t)}\tilde{\psi}(x,t), \tag{4.29}$$

with $V=\partial_t A$. After Fourier transformation this becomes

$$\psi_-(E)=\sum_n c_n\tilde{\psi}_-\left(E-n\omega+\frac{V_{\rm sd}}{2}\right). \tag{4.30}$$

Since the new field, $\tilde{\psi}$, satisfies the free wave equation, $(\partial_t+\partial_x)\tilde{\psi}=0$, for $x<0$, we assume again that it is incident upon the point contact with a Fermi distribution function $f(E)=(\exp(\beta E)+1)^{-1}$. The distribution function for the original fermion, $\langle\psi_-^\dagger(E)\psi_-(E')\rangle=2\pi\delta(E-E')f^{\rm ex}(E)$, is thus given again by the ''excited Fermi function''

$$f^{\rm ex}(E)=\sum_n |c_n|^2 f\left(k-n\omega+\frac{V_{\rm sd}}{2}\right). \tag{4.31}$$

Finally, the backscattered current averaged over time follows from Eq. (4.22) as

$$\langle I_B\rangle_{\rm time}=\tfrac{1}{2}\int\frac{dE}{2\pi}\ \langle\psi_+^\dagger(E)\psi_+(E)-\psi_-^\dagger(E)\psi_-(E)\rangle. \tag{4.32}$$

After reexpressing outgoing waves in terms of incoming, using the S matrix (4.28), the averages over the incident distribution can be performed, giving

$$\langle I_B\rangle_{\rm time}=\int\frac{dE}{2\pi}\ |S_{+-}(E)|^2(\tfrac{1}{2}-f^{\rm ex}(E)). \tag{4.33}$$

The total transmitted current (2.8) can once again be cast into the form

$$I(V_{\rm sd},V_{\rm ac})=\sum_n |c_n|^2 I^{\rm dc}(\nu V_{\rm sd}+n\omega), \tag{4.34}$$

with $\nu=\frac{1}{2}$. Here the current in the absence of ac drive, $I^{\rm dc}(V_{\rm sd})\equiv I(V_{\rm sd},0)$, is given by

$$I^{\rm dc}(V_{\rm sd})=\frac{1}{4\pi}V_{\rm sd}-\int\frac{dE}{2\pi}|S_{+-}(E)|^2(\tfrac{1}{2}-f(E+\tfrac{1}{2}V_{\rm sd})). \tag{4.35}$$

Notice that in contrast to the case $\nu=1$, the S matrix here depends on the energy of the incident fermion. As a result, the I-V curve is non-Ohmic. The differential conductance at zero temperature as obtained from Eq. (4.35) in the absence of the ac drive is plotted in Fig. 4. At small bias, the current vanishes with the cube of the source-drain voltage. This is consistent with the general result $I\sim V_{\rm sd}^{2/\nu-1}$, obtained from perturbation theory in the strong backscattering limit. For large bias the I-V curve is linear with an offset voltage. Again, this is consistent with the general perturbative result for small backscattering; $((\nu/2\pi)V_{\rm sd}-I)\sim v^2V_{\rm sd}^{2\nu-1}$ Notice that for all $\nu<\frac{1}{2}$, the I-V curve at large voltage is thus expected to asymptote to $I=(\nu/2\pi)V_{\rm sd}$, with *no* offset.

With the ac drive present, the I-V curve can be obtained by summing in Eq. (4.34), with weighting $|c_n|^2=J_n^2(V_{\rm ac}/2\omega)$. Since the I-V curve with no ac drive is non-Ohmic at small bias, this will give features in the full I-V curve which resemble smeared current plateaus. These plateaus can be more readily revealed by plotting dI/dV versus $V_{\rm sd}$.

Anticipating the analysis of the I-V curves for general ν in Sec. V, it is convenient at this stage to define an effective backscattering energy or temperature scale. Following Fendley, Ludwig, and Saleur, we define a backscattering temperature $T_B=g(\nu)\omega_c(v/\omega_c)^{1/(1-\nu)}$, where the function $g(x)$ is

$$g(x)=\frac{4\sqrt{\pi}}{x}x^{1/(2-2x)}\left(\frac{1}{x}-1\right)^{1/2}\frac{\Gamma\left(\dfrac{1}{2-2x}\right)}{\Gamma\left(\dfrac{x}{2-2x}\right)}. \tag{4.36}$$

In the $\nu\to0$ limit, one has $T_B=2\pi v$, which is the appropriate backscattering energy scale entering in the semiclassical equations of motion (3.17). For $\nu=\frac{1}{2}$, $T_B=4v^2/\omega_c$, which is the energy scale that enters in Eq. (4.28). The I-V curves at $T=0$ are then characterized by two dimensionless parameters $\nu\tilde{V}_{\rm ac}=\nu V_{\rm ac}/\omega$ and $\nu\tilde{T}_B=\nu T_B/\omega$.

In Fig. 5 we plot the differential conductance versus voltage, obtained from Eq. (4.34) with $\nu\tilde{V}_{\rm ac}=1.6$ and $\nu\tilde{T}_B=\frac{1}{4}$. Notice the minima, which correspond to smeared plateaus in the I-V curves. The differential conductance at the nth

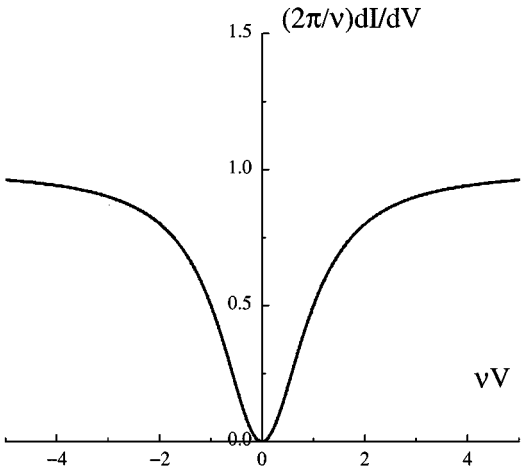

FIG. 4. Differential conductance with no ac drive at $\nu=\frac{1}{2}$. We choose $\nu T_B=1$ in this plot.

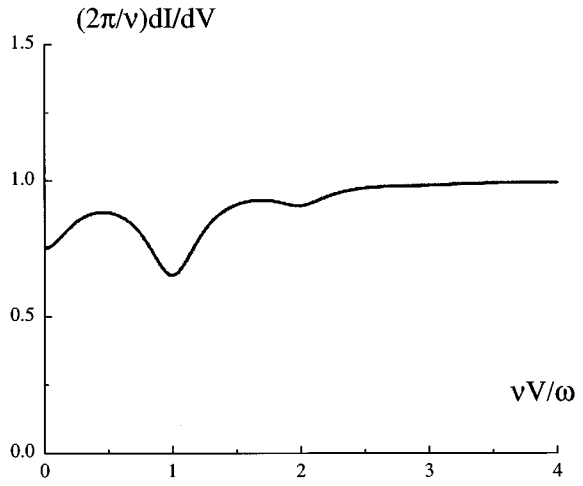

FIG. 5. Differential conductance with ac drive at $\nu=\frac{1}{2}$ obtained from Eq. (4.34), plotted versus voltage. We have put $\nu T_B=\omega/4$, and $\nu V_{\rm ac}=1.6\omega$. The minima correspond to smeared plateaus in the I-V curve, centered around $\nu V_{\rm sd}=n\omega$.

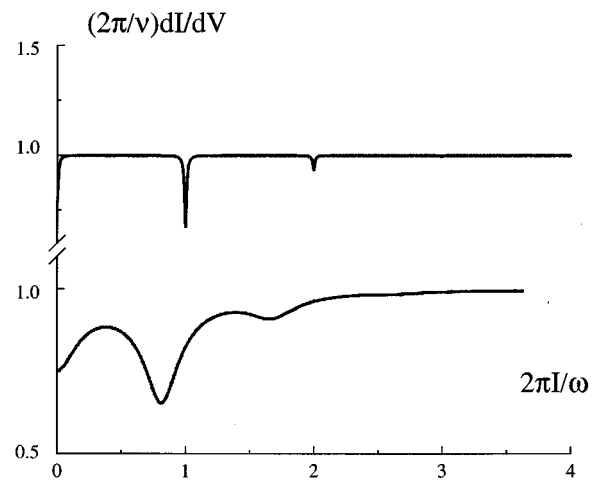

FIG. 6. Differential conductance with ac drive at $\nu=\frac{1}{2}$ at two different backscattering strengths. In the lower part of the figure, we plot the same differential conductance as in Fig. 5 but vs current. As one can see that the smeared plateaus are *not* centered at $I=ne\omega/2\pi$ due to the finite offset. In the upper part, we put $\nu T_B=\omega/100$ and $\nu V_{\rm ac}=1.6\omega$. In this weak backscattering limit, the ''plateaus'' are centered at the quantized values $I=ne\omega/2\pi$.

minima is $1-J_n^2(V_{\rm ac}/2\omega)$. The widths of the minima depend primarily on the backscattering energy scale T_B, becoming narrower as T_B decreases. In contrast to the semiclassical approximation (3.17), the ''plateaus'' here have a nonvanishing differential conductance everywhere—they are not ''flat.'' Moreover, the I-V curve is analytic everywhere, even at the ''plateau'' centers, since the I-V curve without ac drive is analytic even at zero bias. Evidently, quantum fluctuations are quite effective at smearing the semiclassical current plateaus, even for $\nu=\frac{1}{2}$.

It is also instructive to plot the differential conductance, dI/dV, versus the current, as shown in Fig. 6. This shows clearly that the smeared ''plateaus'' are not centered at the quantized current values $I=ne\omega/2\pi$. This is due in part to the finite offset voltage at large bias, mentioned above. However, if we choose a smaller backscattering strength, $T_B\to 0^+$, these ''plateaus'' become centered at the quantized current values, $I=ne\omega/2\pi$, as shown in Fig. 6. We next consider the I-V curve for general ν.

V. GENERAL ν

In Sec. IV we showed that for both $\nu=1$ and $\nu=\frac{1}{2}$, the I-V curve with ac drive, could be related to the I-V curve in the absence of any ac drive, as a weighted sum over absorption and emission of quanta, see Eq. (4.34). Here we make the conjecture that this relation holds in general, for arbitrary ν. If correct, this conjecture allows us to use the recent results of Fendley, Ludwig, and Saleur[15] to extract I-V curves with ac drive for *arbitrary* integer ν^{-1}. Before doing so, we show that the conjecture does hold for general ν in the limit of weak backscattering.

To this end, consider calculating the I-V curve with ac drive present, as a perturbation expansion in powers of the backscattering amplitude v. The leading nonvanishing correction appears at order v^2. This correction can be readily obtained from the Keldysh action discussed in Sec. III. The backscattered current operator follows from Eq. (3.6) upon functional differentiation with respect to the gauge field $A(t)$,

$$\hat{I}_B=\nu v\ \sin(\theta+\nu A). \tag{5.1}$$

Within the Keldysh approach, the average over this operator can be performed by putting it into the forward path, so that

$$\langle I_B\rangle=\langle\sin(\theta_+(t)+\nu A)\rangle, \tag{5.2}$$

where the average is taken with respect to the generating functional (3.7). Upon expanding the exponential $\exp(-S_1)$ to second order in v, one obtains

$$I_B=-\frac{i}{2}\nu v^2\int dt' \times\langle\sin[\theta_+(t)-\theta_-(t')+\nu(A(t)-A(t'))]\rangle_0, \tag{5.3}$$

where the subscript 0 denotes an average with respect to the quadratic action S_0 in Eq. (3.9). Keeping only the constant time-independent piece, it is then straightforward to show that

$$\langle I_B\rangle_{\rm time}=\sum_n\ |c_n|^2\ \ I_B^{\rm dc}(\nu V_{\rm sd}+n\omega), \tag{5.4}$$

where $I_B^{\rm dc}$ is the backscattered current to order v^2 without the ac drive. Since the total current is $I=\nu V_{\rm sd}-I_B$, the sum rule $\Sigma_n|c_n|^2=1$ can be used to verify the general conjecture (1.1). A similar expression for the current under ac drive in small backscattering regime was obtained before by Wen.[1]

The general conjecture has a very simple and physical interpretation. In the absence of an ac drive, Laughlin quasiparticles with fractional charge ν lose an energy $\nu V_{\rm sd}$ when they backscatter from one edge to the other. With ac drive, the quasiparticles absorb or emit quanta of energy $\hbar\omega$ from the ac drive, and jump into different energy levels $\nu V_{\rm sd}\pm n\omega$, with probability $|c_n|^2$. They are then backscattered by the point contact, with a reflection coefficient given by the energy-dependent S matrix. This contributes a backscattered current $I^{\rm dc}(\nu V_{\rm sd}\pm n\omega)$. The total backscattering follows by summing over the number of absorbed quanta n, weighted with the probability $|c_n|^2$.

In the absence of an ac drive, the I-V curve can be extracted from the exact solution of Fendley, Ludwig, and Saleur. We can then use the general conjecture to evaluate explicitly the I-V curve with ac drive for the Laughlin FQHE states. It is interesting to compare the results in the $\nu\to 0$ limit with a semiclassical model in Sec. III. Using the exact solutions of Fendley, Ludwig, and Saleur, it is possible to take the $\nu\to 0$ limit. If we keep $\nu V_{\rm ac}$, $\nu V_{\rm sd}$, and νT_B fixed as $\nu\to 0$, then the I-V curve (with no ac drive), reduces to that obtained from the classical equation of motion (3.17). This solution is shown in Fig. 7. With ac drive present, the I-V curves in the $\nu\to 0$ limit can be extracted from our conjecture, and are shown in Fig. 8. Notice that these I-V curves do *not* coincide with the solutions of the classical equation of

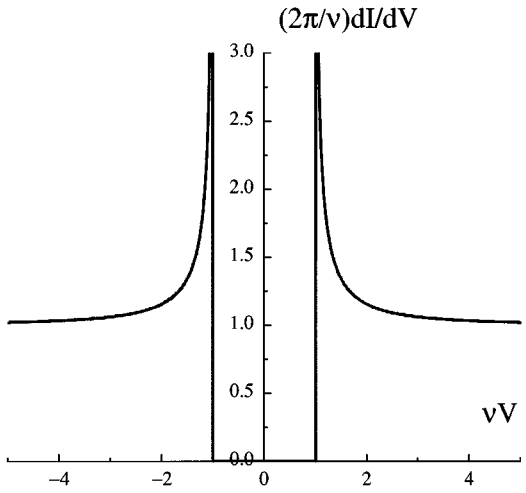

FIG. 7. Differential conductance with no ac drive present in the $\nu \to 0$ limit with $\nu T_B = 1$ fixed, as obtained from the exact solution of Fendley, Ludwig, and Saleur. This *I-V* curve is identical to that obtained from the classical equation of motion (3.17). Below a threshold voltage there is *no* electron tunneling.

motion (3.17), plotted in Fig. 2. Specifically, they do *not* exhibit flat mode-locked plateaus, in contrast to Fig. 2. As discussed at the end of Sec. III, the reason for this can be attributed to the presence of two parallel quantum processes which facilitate electron transfer: tunneling under the barriers, and over the barrier motion after quantized energy absorption from the ac field. In the $\nu \to 0$ limit, only the first process is suppressed. However, in the classical limit (3.17), both quantum processes are absent. The second quantum process is evidently responsible for smearing the current plateaus, and spoiling the precise quantization.

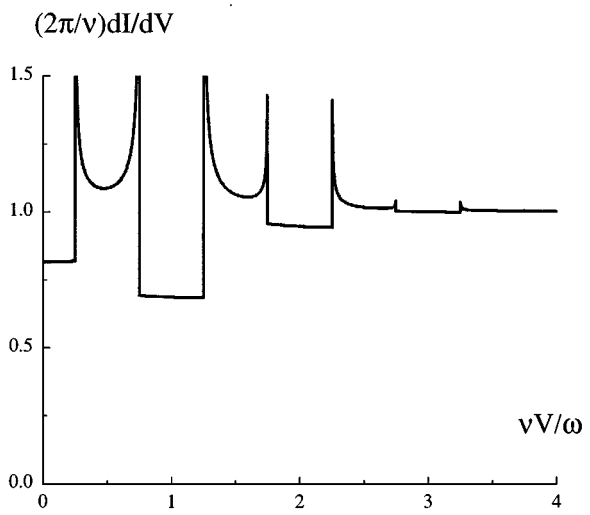

FIG. 8. Differential conductance with ac drive present obtained from the conjecture (1.1), in the $\nu \to 0$ limit with $\nu T_B = \omega/4$ and $\nu V_{ac} = 1.6\omega$ held fixed, plotted vs voltage. In contrast to the classical solution from Eq. (3.17) shown in Fig. 2, the above-current ''plateaus'' are rounded by quantum fluctuations.

VI. DISCUSSION AND CONCLUSIONS

Electron turnstile devices which transfer electrons one by one have been made both in metals[6–8] and in semiconductors.[9–11] These devices consist of multiple-tunnel junctions in series. By selectively controlling the junction barrier heights, a single electron at a time can be transported through the device. By applying an ac drive field to the barriers, with an appropriate phase relationship between successive junctions, it is possible to transport one electron through the device for each period of the ac drive. This leads to a plateau in the current-voltage characteristics at the quantized value $I = e\omega/2\pi$, with ω the ac drive angular frequency. These devices work well only at relatively low frequencies (MHz). At higher frequencies, the electrons do not ''keep up'' with the ac drive.

A key feature of the turnstile devices appears to be the multiple-junction geometry. The electron being transported through the device presumably suffers numerous inelastic scattering events while on the islands between junctions. These phase-breaking events destroy the electron coherence, effectively making the electron dynamics classical and suppressing leakage from quantum tunneling. In this way quantum fluctuations do not destroy the mode locking to the external ac drive.

In this paper, we considered a point-contact tunnel junction between two quantum Hall fluids. In contrast to the turnstile devices, the junction has only one barrier. The electron is assumed to tunnel coherently through the barrier, suffering only inelastic collisions in the ''contacts'' (i.e., in the edge states) on either side of the barrier. Moreover, we assume the transmission amplitude through the barrier to be independent of energy. Within a semiclassical approximation to this model, there are robust quantized current plateaus in the presence of an ac drive field, similar to that seen in the turnstile devices. However, inclusion of quantum fluctuation effects tends to smear these plateaus. Specifically, for the IQHE at filling $\nu = 1$, where the edge state is a free-fermion gas, the *I-V* curve with ac drive is strictly Ohmic and featureless. Mode-locked plateaus in the current are completely destroyed by quantum fluctuations.

In the FQHE the edge states are Luttinger liquids. In this case, even though the bare tunneling amplitude through the point contact is energy independent, interaction effects in the edge-state ''leads'' give an energy dependence to the total tunneling rate. (The tunneling rate vanishes as a power law of energy, for energies close to the Fermi energy.) In this case, with an ac drive present, the *I-V* curves do exhibit features, which can be identified as mode-locked current plateaus rounded by quantum fluctuations. However, the ''plateaus'' are *not* completely flat—the current varies upon sweeping the voltage. In the limit of weak backscattering at the point contact, the rounded plateaus are centered at currents given by integer multiples of $I = e\omega/2\pi$, as shown in Fig. 6.

What are the prospects for using FQHE tunnel junctions as a current to frequency standard? The prediction of rounded current plateaus induced by the ac drive—centered at quantized values $I = ne\omega/2\pi$ for weak backscattering—is encouraging. However, since the ''plateaus'' are *not* completely flat, the degree of current quantization will necessarily be limited. Whether this fundamental limitation renders

the device useless is difficult to assess. In a practical device, the quantization could presumably be improved upon, by making multiple FQHE junctions, similar to the semiconductor turnstiles. In any event, it would be fascinating to explore experimentally the effects of an ac drive on quantum Hall point contacts.

ACKNOWLEDGMENTS

We thank A. Ludwig, S.M. Girvin, and Paul Fendley for clarifying conversations. We are grateful to the National Science Foundation for support under Grant Nos. PHY94–07194, DMR–9400142, and DMR-9528578.

[1] X. G. Wen, Phys. Rev. Lett. **64**, 2206 (1990); Phys. Rev. B **41**, 12 838 (1990); **43**, 11 025 (1991); **44**, 5708 (1991).
[2] K. Moon, H. Yi, C. L. Kane, S. M. Girvin, and M. P. A. Fisher, Phys. Rev. Lett. **71**, 4381 (1993).
[3] F. P. Milliken, C. P. Umbach, and R. A. Webb, Solid State Commun. **97**, 309 (1996).
[4] S. Shapiro, Phys. Rev. Lett. **17**, 166 (1963).
[5] E. Ben-Jacob and Y. Gefen, Phys. Lett. **108A**, 289 (1985).
[6] L. J. Geerligs, V. F. Anderegg, P. A. M. Holweg, J. E. Mooij, H. Poyhier, D. Esteve, C. Urbina, and M. H. Devoret, Phys. Rev. Lett. **64**, 2691 (1990).
[7] L. J. Geerligs, Surf. Sci. **263**, 396 (1992).
[8] J. D. White and M. Wagner, Phys. Rev. B **48**, 2799 (1993).
[9] L. P. Kouwenhoven, A. T. Johnson, N. C. van der Vaart, C. J. P. M. Harmans, and C.T. Foxon, Phys. Rev. Lett. **67**, 1626 (1991).
[10] L. P. Kouwenhoven, A. T. Johnson, N. C. van der Vaart, and D. J. Maas *et al.*, Surf. Sci. **263**, 405 (1992).
[11] Y. Nagamune, H. Sakaki, L. P. Kouwenhoven, and L. C. Mur *et al.*, Appl. Phys. Lett. **64**, 2379 (1994).
[12] D. E. McCumber, J. Appl. Phys. **39**, 2503 (1968); **39**, 3113 (1968).
[13] W. C. Stewart, Appl. Phys. Lett. **12**, 277 (1968).
[14] W. J. Johnson, J. Appl. Phys. **41**, 2958 (1968).
[15] P. Fendley, A. W. W. Ludwig, and H. Saleur, Phys. Rev. B **52**, 8934 (1995).
[16] C. L. Kane and M. P. A. Fisher, Phys. Rev. B **46**, 15 233 (1992).
[17] M. Stone and M. P. A. Fisher, Int. J. Mod. Phys. B **8**, 2539 (1994).
[18] P. Fendley, A. W. W. Ludwig, and H. Saleur, Phys. Lett. B **338**, 2379 (1994).
[19] M. H. Jensen, Per Bak, and Tomas Bohr, Phys. Rev. Lett. **50**, 1637 (1983).
[20] A. O. Caldeira and A. J. Legget, Ann. Phys. (N.Y.) **149**, 374 (1983).
[21] M. P. A. Fisher and W. Zwerger, Phys. Rev. B **32**, 6190 (1985).
[22] P. C. Martin, E. D. Siggia, and H. A. Rose, Phys. Rev. A **8**, 423 (1973).
[23] C. A. Hamilton, Rev. Sci. Instrum. **43**, 445 (1972).
[24] P. Russer, J. Appl. Phys. **43**, 2008 (1972).
[25] H. D. Hahlbohm, A. Hoffmann, H. Lübbig, H. Luther, and S. Seeck, Phys. Status Solidi A **13**, 607 (1972).
[26] M. Ya. Azbel and Per Bak, Phys. Rev. B **30**, 3722 (1984).